Kuwait J.Sci., Vol.48, No.(4),October.2021,pp(1-12)

Flow characterization near the nozzle exit of the supersonic steam jet injecting into the stagnant water

Afrasyab Khan[1,*], Khairuddin Sanaullah[2], Mohammed Zwawi[3], Mohammed Algarni[3], Bassem F. Felemban[4], Ali Bahadar[5], Ahmed Salam Farooqi[6]
Andrew Ragai Henry Rigit[7], Atta Ullah[8]

[1]*Institute of Engineering and Technology, Dept. of Hydraulics and Hydraulic and Pneumatic Systems, South Ural State University, Lenin Prospect 76, Chelyabinsk, 454080, Russian Federation.*
[2] *Dept. of Chemical Engineering & Energy Sustainability, Faculty of Engineering, University Malaysia Sarawak (UNIMAS), 94300 Kota Samarahan, Sarawak, Malaysia.*
[3] *Dept. of Mechanical Engineering, King Abdulaziz University, Rabigh 21911, Saudi Arabia.*
[4]*Mechanical Engineering Department, Taif University, Taif 26571, Saudi Arabia.*
[5] *Dept. of Chemical and Materials Engineering, King Abdulaziz University, Rabigh 21911, Saudi Arabia.*
[6] *Dept. of Chemical Engineering, Universiti Teknologi Petronas, Bandar Seri Iskandar, 32610, Perak, Malaysia.*
[7] *Dept. of Mechanical and Manufacturing Engineering, Faculty of Engineering, University Malaysia Sarawak (Unimas), 94300 Kota Samarahan, Sarawak, Malaysia.*
[8] *Dept. of Chemical Engineering, Pakistan Institute of Engineering & Applied Sciences (PIEAS), Nilor, Islamabad, Pakistan.*
[*]*Corresponding author: khana@susu.ru*

Abstract

There has been a large amount of work being conducted on the thermo-dynamics of the Direct Contact Condensation (DCC), however, not much attention was given to the phenomena particularly active near the steam's nozzle exit. A transparent rectangular upright duct of 4 ft high, was built with a supersonic nozzle positioned at the bottom of the channel to characterize flow behavior near the steam nozzle's exit. Particle image velocimetry (PIV) was applied to draw information on the steam's jet penetration into the water as well as the entrainment and mixing between the two phases under the steam's inlet pressure ranging from 1.5 – 3.0 bars. PIV normalized contour measurements depicted not appreciable changes in the radial velocity of the jet. Whereas, in the core region of the jet, the change in the jet's velocity was not much till Y/De ~ 4.3 and the vertical velocity of the jet decreased slowly till Y/De ~ 8. The jet's normalized upward velocity attained an optimized value between Y/De ~ 8 and Y/De ~ 9.8. With varying pressures, 1.5 bars to 3.0 bars, the jet expanded radially in water. It was also found in the near nozzle exit region, the shear layer's thickness remained within 0.2 – 0.5 De over the 1.5 – 3.0 bars pressure. Probability Density Function (PDF) analysis of Reynolds shear and normal stresses confirmed the existence of the velocity fluctuations across the shear layer, owing to the large eddies across the steam-water interface.

Keywords: Hydrodynamics; local and core circulation; pulsating injection; *steam*-water flow; vortical Structure.

1. Introduction

When the steam is discharged into the pool of water, Direct Contact Condensation (DCC) occurs, which relies on the transfer of heat as well as the mass of the steam into the water. Till date, a huge amount of work has been devoted to the thermal-hydraulic aspects of the phenomena of the DCC, that includes the research on the jet's shape and length, mass and heat transfer, and the flow instabilities associated with the DCC phenomena (Afrasyab *et. al.*, 2013; Chun *et. al.*, 1996; Khan

et. al., 2016, Song, Chul-Hwa 2007; Cho, Seok; Kim, Hwan-Yeol; Bae, Yoon-Young; Chung, 2000, n.d.; Weimer *et. al.*, 1973). The supersonic steam's jet injection has myriad uses in the safety studies that are related to nuclear power, where this phenomenon contributes significantly to the storage of water, which serves the role of a heat sink as a result of dumping of the steam that has been discharged from the Reactor Coolant System (RCS) (Song, Chul-Hwa 2007; Cho, Seok; Kim, Hwan-Yeol; Bae, Yoon-Young; Chung, 2000).

The region just outside the nozzle exit of the injecting steam's jet into the still water is very significant and understanding of flow characteristics in this region is vital to elaborate the overall significance of the steam's jet interaction with the surrounding water. The region has the lower pressure and thus offers a higher suction of the surrounding fluids into the region. The physical picture of the steam's jet near the nozzle exit reveals that the higher density of the steam near the exit initially with the jet itself has a the positively buoyant nature. However, the jet entrains the water from the surroundings as it moves further from the exit. The density difference between the two phases reduces, and in the end with a constant dwindling profile, the jet terminates after being penetrated for some distance along the direction of injection.

The modeling of the turbulent jets and plumes associated with the steam's injection into the pool of water can conveniently be performed with the help of the entrainment ratio, which is conveniently referred to as the ratio of the radial velocity of the surrounding fluid towards the axial jet to the jet's velocity at the radial distance equal to the half of axial axis of the jet velocity (Zong *et. al.*, 2016). The typical empirical values obtained for the ratio were 0.054 for the jets and 0.09 for the plumes, which reasonably provided a reasonable estimate using modeling approaches (Yang *et. al.*, 2019). In the case of the supersonic steam jet injection into the subcooled water, the jet at the most can penetrate several diameters of the steam's nozzle exit, whereas the shear layer is quite thinner in most of the cases with the eddies being able to drive the entrainment process through the shear layer (Yang *et. al.*, 2015). There is amply literature that cites the entrainment of the surrounding fluid as a result of a jet injection into it, for instance, the extent of entrainment along with turbulence dissipation associated with the swirl steam injection into the water (Khan *et. al.*, 2019). Few studies that comprised of the PIV study of the gas that exited from an orifice into the flat plate, in comparison to its exits from the smoothed contoured nozzle with its exit from the long pipe (Mi *et. al.*, 2007). The significant observation drawn from this study revealed that the turbulence was not fully developed even after 16 diameters of the orifice/nozzle/pipe exit, however, the mean-field approached a self-similar Gaussian profile. However, downstream expansion and contraction waves prevailed throughout the fluid domain wherever steam interacted with the surrounding water. These waves were generated due to the inception and collapse of the steam bubbles within the surrounding water. In the case of the compressible fluids, the region being inhibited these compression and expansion waves, which has been dominated by the density contrast fluid domains, i.e. steam and water due to which the entrainment has been reduced along the axial direction across the interface which affects the mass flow rate of these fluids. Whereas, in the case of the moderately overpressure jets the entrainment was reduced to around 50% due to the compressibility effects (Solovitz *et. al.*, 2011). In another study, the importance of the density gradient within the two parallel streams of the fluids has been determined, with major attention on the growth of the interacting layer between the two. The striking finding from this study revealed that the density gradient itself was not enough alone to describe the reduction in the mixing growth layer in the compressible fluids. In addition to it, one couldn't ignore the velocity and pressure fluctuations which contributed mainly towards the Mach number among these flows (Brown & Roshko, 1974). Also, the mixing layer growth was obtained by using the Schlieren images and traversing pitot tubes and it was found to be dependent on the convective Mach number because the propagation of the flow disturbances was proportional to the Mach number (Papamoschou & Roshko, 1988).

Among the studies mentioned here, only a few have emphasized the entrainment of the surrounding fluid by the jets/plumes in the developing regions. Still, none of the studies precisely shed light on the flow hydrodynamics in the region adjoining to the nozzle exit as well as the entrainment issues and the physics prevailed within the region close to nozzle exit in the case of the supersonic steam jet injection into the subcooled water. The experimental setup, involving a rectangular vertical glass column with a supersonic nozzle fitted at the bottom of the column, was used to characterize flow within a region adjacent to the nozzle's exit by the application of the PIV technique. The details of the experimental setup and the measurements conducted by utilizing the PIV are illustrated in the following sections.

2. Experimental setup

The experimental setup was comprised of a rectangular vertical glass vessel having the dimensions (length, L = 2 feet, height, H = 4 feet, and width, W = 2 feet) filled with water up to 3.8 feet. The supersonic nozzle was inserted at the base of the rectangular vessel. The nozzle has the dimensions (length = 10 cm, length of the chamber = 2 cm, length of converging section = 8.5 cm, length of the diverging section = 2.2 cm, diameter of the throat = 0.2 cm, diameter of the exit, De = 0.3 cm, inlet diameter = 2 cm) as shown in Figure 1. Velocity measurements were obtained by using a PIV system. The PIV consisted of a charged coupled diode camera with resolution 2048 x 2048~ 7.4 pixels. The laser had a pulse with a National instruments data acquisition and frequency of ~15 Hz and power 200 mJ/pulse data processing software module. Fluorescent 1.0 g/cc microspheres were used as tracer particles, which faithfully followed the fluid streams because of having nearly same density as of the fluid.

Data was acquired for 10 minutes at a rate of 10 Hz. Thus, using this configuration, 6000 frames were acquired in 10 minutes against a single operating condition. The frame for the CCD camera was adjusted in such a way that it only focused on the area exactly surrounding the

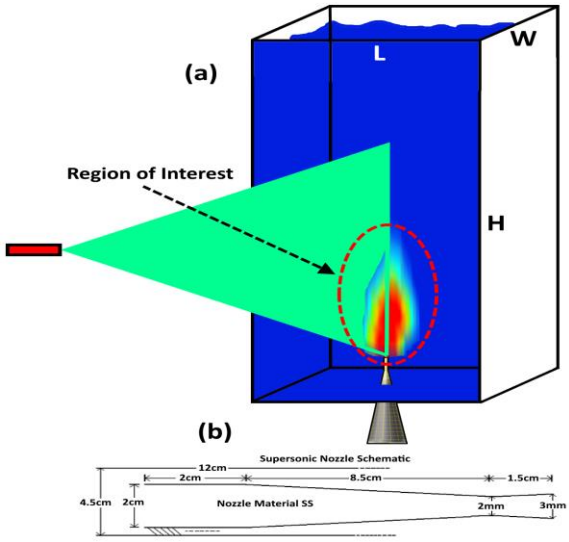

Fig. 1. A schematic of an experimental setup and supersonic nozzle**,** (a) Experimental Setup (b) Supersonic nozzle.

nozzle exit as shown by the dotted circle in Figure 1. From the generated frames anomaly detection was performed to remove the uneven data points from the PIV frames. The calibration of the PIV was performed by using method for the accurate measurement of the laser pulse magnification and separation. The pulse separation was measured by focusing the laser sheet on the photodetector which itself was connected to the oscilloscope which provided of how much separation existed with respect to the distance between the point of light emergence and the point of light incidence on to the photodetector.

The magnification-related errors were determined by focusing the laser sheet light on a known grid dimension, following this, the ratio of the measured grid spacing with the known grid spacing was adopted. This helped to estimate the extent of the optical distortions. In case of zero distortion, the ratio value remained the same at all the locations along with the fluid domain. The measured uncertainties for the present experimental setup were 0.1 - 0.3%. The profiles obtained from the PIV techniques were converted into black and white images by application of the decolorization technique with contrast preserving measures (Zhao *et. al.*, 2018) as well as edge detection technique through

Matlab (Matlab, n.d.). This relaxed the contrast of the colour constraints, using these to construct the non-local colour pair (white & black) by applying the non-linear bounding hierarchy in which the duplication of the local colour was removed.

3. Results & discussion

In this study, the supersonic steam jet was injected into the subcooled water in a vertical orientation. The inlet pressure of the steam was varied from 1.5 - 3.0 bars. The flow dynamics in the region adjacent to the nozzle exit have been discussed in detail in the following sections. The details of the results in this regard are given as follows.

3.1 Hydrodynamics of the supersonic steam in the regions near the nozzle exit

The flow structures based upon the normalized velocity contours were characterized here. The velocity was normalized by the jet's centerline velocity at the exit. At an inlet pressure of 1.5 bars, the jet exited the nozzle at an approximate uniform velocity, thus generating a shear layer that acted upon the surrounding water into a growing behavior along the axial as well as radial directions as shown in Figure 2. The colored PIV images were transformed into black and white images of high resolution, the intensity of the resolution can be visible from the Figure 2 and Figure 3. As seen from these figures, the moment the jet exits the nozzle, the radial interfaces with the water have shown a very little growth, however, the radial spread of the jet gradually increases due to more surrounding water being entrained, as the jet moves vertically upward. Whereas the jet's velocity within the core region remains unchanged till Y/De ~ 4.3, further distance from this, the jet centerline velocities have shown a gradual decrease.

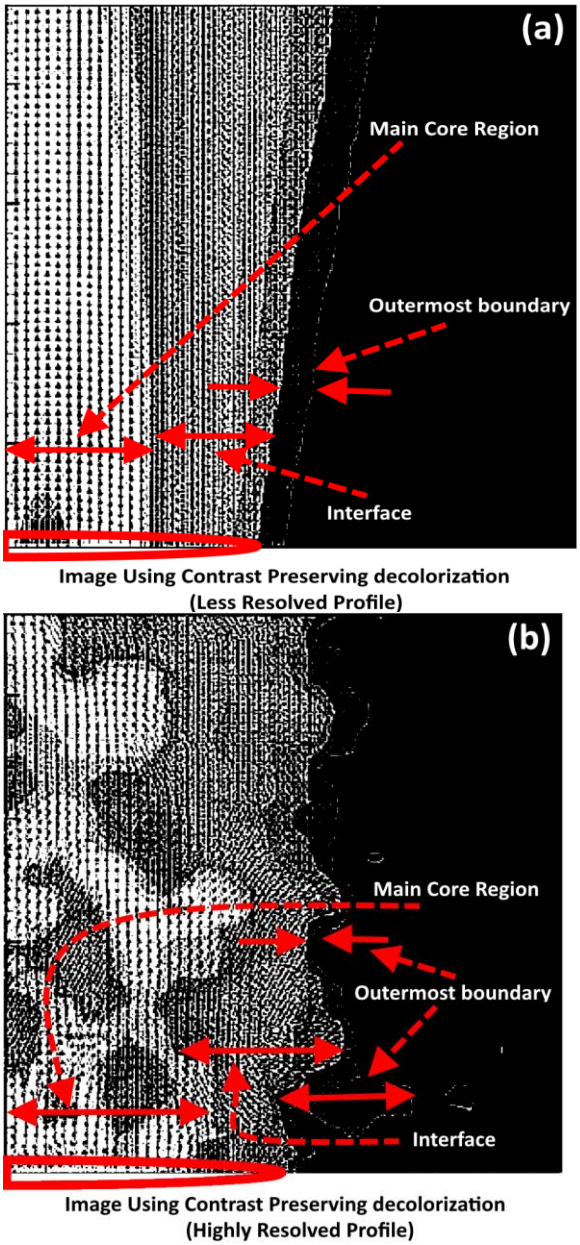

Fig. 2. Contrast preserving decolorization images for the regions near the nozzle's exit.

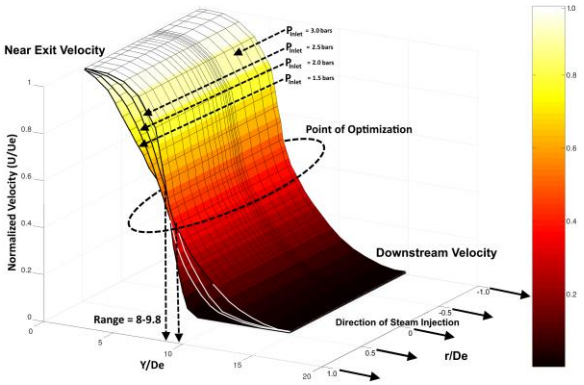

Fig. 3. Plot between normalized axial distance and normalized axial velocity distribution.

The trends being presented here were due to the contours of the jet velocities from the nozzle exit till the downstream point of observation, see Figure 3. It should be noted that these profiles were based upon the velocity values across the jet, r/De = 0 - 1.0. The velocity was normalized by the steam jet's exit velocity, Ue, whereas the axial and radial distances were normalized by

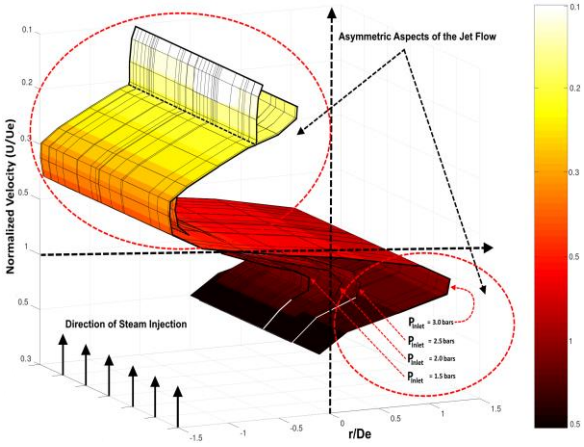

Fig. 4. Plot between normalized radial distance and normalized radial velocity distribution (asymmetric aspects of the flow) in the regions near the nozzle exit.

the diameter of the nozzle exit, De. The jet's exit velocity shows initially a gradually decreasing behaviour till Y/De = 8, however, further from this till Y/De = 9.8, the jet's exit velocity has shown an optimized behaviour. The optimized profile implies that the velocities of the jet match with each other irrespective of the steam's inlet pressure. The profiles within the developing region grow with the spread of the shear layer. Among the compressible fluids, which were representative of considerable mass transfer, the steam-water flows didn't need any higher distances to become fully developed, contrary to the non-condensable fluids like air-water flows (Mi *et. al.*, 2007), rather the velocity profiles exhibited a non-conserving momentum outcome. It was observed that varying the pressure from 1.5 - 3.0 bars of inlet pressure, the jet widened in the water at atmospheric pressure. The velocity close to the exit region has higher values than the velocity at the same location at lower inlet pressure, this was due to the reason that the steam expanded as it came out of the exit of the nozzle. The sudden expansion experienced by the steam resulted in a lowering of the pressure in the exit region along with the rise in the velocity in the exit region (Khan *et. al.*, 2014). The velocity field was further analyzed in the near exit locations at multiple positions (0 - 5De) as shown in Figure 4.

The steam's jet exiting the nozzle at the supersonic speed, which dissipates as soon as it penetrates the water in the vertically upward direction. The flow shows an asymmetric behavior right from the exit of the nozzle and quickly this asymmetric behavior propagates downstream of the nozzle exit.

The compression and expansion waves inherent in the supersonic steam jet's injection into the water cause the velocity profiles imbalance across the axial position, of the nozzle, the asymmetry was observed in a number of other studies related to the supersonic steam injection into the water. Overall, across the axial position the steam jet has shown a Gaussian profile. As seen in Figure 4, outside the core region where the jet has shown the slowly varying velocities along the radial direction, the jet velocities have shown a decreasing behaviour even in the flow developing regions. This result is an indication of the influence on the flow due to the entrainment of the surrounding fluid into the jet layer at the expense of the dissipation of the jet's momentum and its kinetic energy.

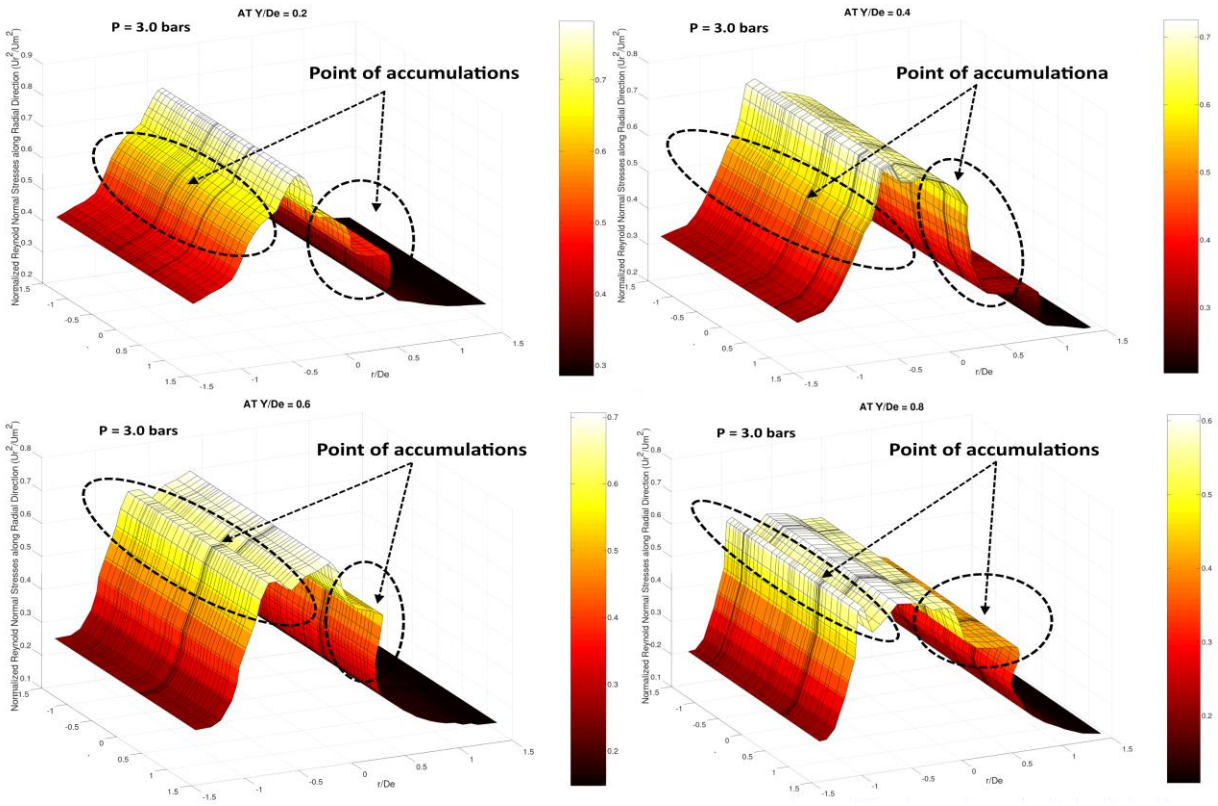

Fig. 5. Plot between normalized Reynolds normal stresses and normalized radial distance.

It should be noted that at the lower inlet pressure, the entrainment was mainly initiated by the central core region velocities, since, the core velocities provided more energy to the eddies that contributed towards the entrainment of the surrounding fluid. However, In the case of the higher pressure jets, the eddies were not directly driven by the core velocities, rather the local velocities were enough to drive such entrainment inhibiting eddies (Brown & Roshko, 1974). Overall, it has been observed that in the near exit region, the shear layer grows in thickness gradually, whereas the difference between their thicknesses never exceeds 0.2-0.5 De in the downstream regions, which almost appears the same on a general basis. The similarity of the thickness of the shear layer may be attributed to our inability in characterizing the steam jet interface precisely as well as its highly fluctuating nature and high-frequency occurrences of the Kelvin Helmholtz instabilities being generated at the interface and then being propagated further into the surrounding water.

3.2 Reynolds shear and normal stresses in the region near the nozzle exit

The velocity fluctuations-based Reynolds shear and normal stresses were measured along the vertical and radial directions by first taking the time average of the ensembled averages at a point and then subtract it from the instantaneous value of the velocities at the location. The Reynolds normal stress, $\overline{u'^2_r}$ and the Reynolds shear stress, $\overline{u'_y u'_r}$ were normalized by the time-averaged core velocities, $\overline{U_m^2}$.

At the lower pressure, and along the radial direction, the normal shear stresses were accumulated in the region where the shear layer originated and started propagation, which was accompanied by large-scale fluctuations due to

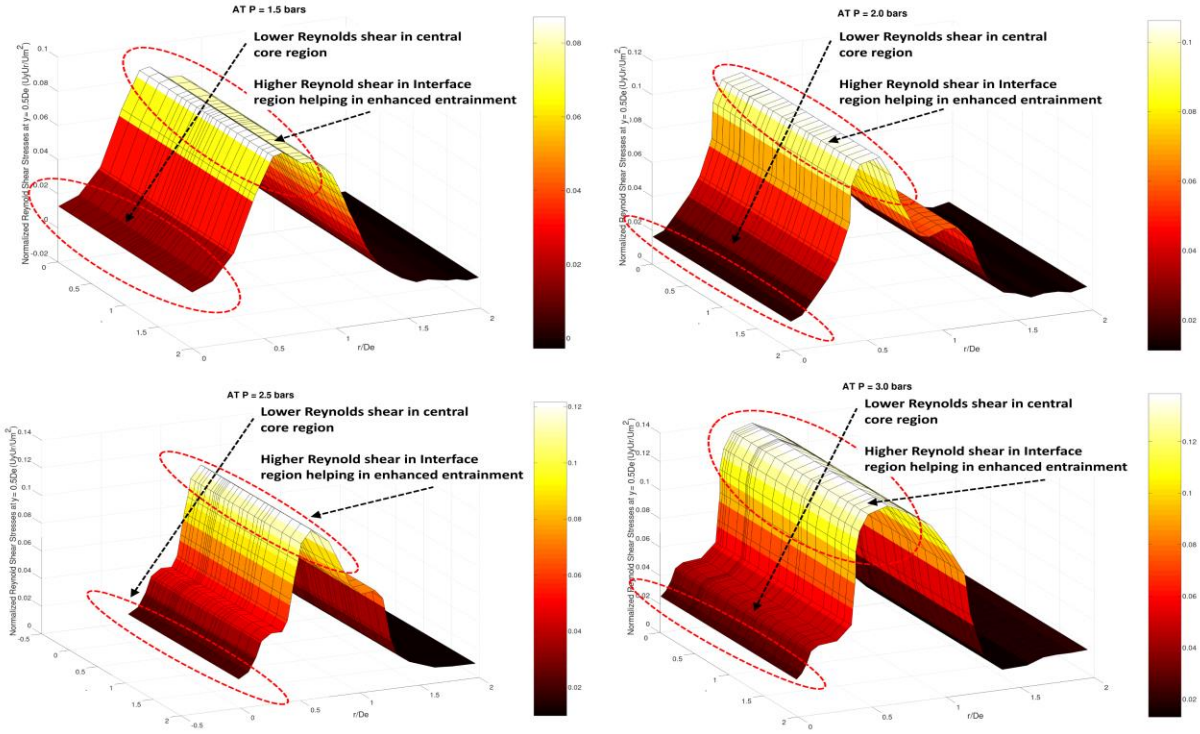

Fig. 6. Plot between normalized Reynolds shear Stresses along normalized radial distance.

the expansion in the shear layer. Along the axial direction, these fluctuations were found to increase with the rise in their amplitudes. In the case of the higher inlet pressure, the radial normal stresses were first accrued in the region marked by the point of initiation of the shear layer with higher values of the normal stresses than their values at the lower pressure which may mainly be attributed to the higher jet velocities at higher inlet pressure. However, along the axial direction, the amplitudes of these fluctuations in the case of the higher pressure became almost comparable to the amplitudes of the fluctuations in the case of the lower pressure. Such behavior may be due to the existence of the optimization point as shown by the results in Figure 5. Since the profiles that have been plotted in this figure were obtained at a pressure of 3.0 bars, whereas the profiles obtained at other pressures also showed almost the same approximate behavior (see Figure 6). In the case of the Reynolds shear stresses at the same location, the profiles have shown a comparable height in comparison to the profiles for the Reynolds stresses. Rather a minor difference can be seen in terms of the larger spatial span of the profiles across the spatial locations.

The Reynolds shear and normal stresses profiles obtained across the flow development regions represent higher amplitudes associated to the velocity fluctuations (Papamoschou & Roshko, 1988). The values of the shear stresses appeared to be very low in the core region along with the axial positions which may be due to a number of reasons, as in the core region the interaction between the jet and the surrounding fluid is almost negligible, secondly, the fluctuation in the core region may be too much frequent so that it may be difficult to characterize such fluctuations precisely. Besides, the nature of such fluctuations may be too minor due to the lower amplitudes of the velocity fluctuations (Urban & Mungal, 1997).

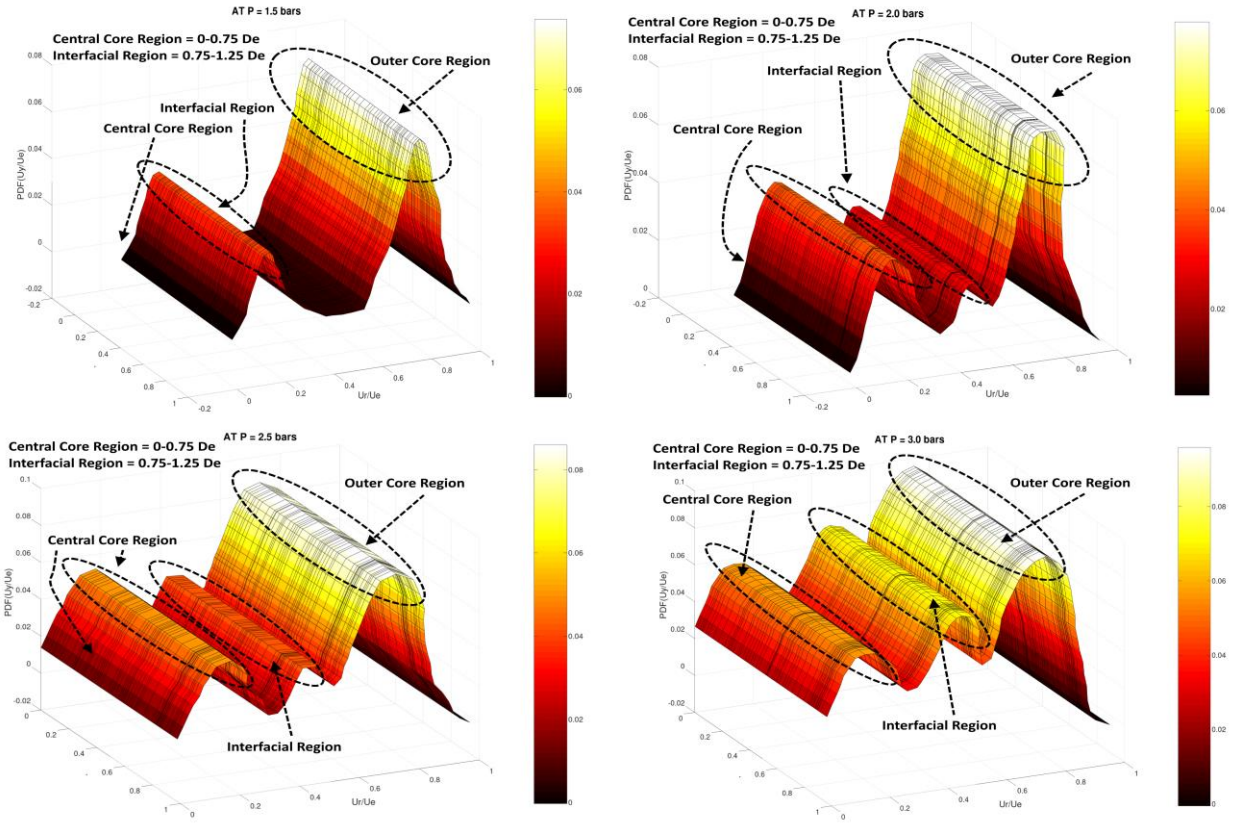

Fig. 7. Probability Density Function analysis of the fluctuating velocity.

In addition, based on the order of magnitude analysis, the growth rate of the shear layer was affected directly by the Reynolds stresses and inversely by the Mach number (Brown & Roshko, 1974).

3.3 Extent of entrainment in the region near the nozzle exit

Here, the effect of the pressure on the entrainment in the regions near the nozzle exit was explored by presenting the variations in the instantaneous velocities. The PDF analysis provides the density of the instantaneous velocity fluctuations across the radial directions with varying inlet pressure. The variations in the instantaneous velocity fluctuations being observed across the shear layer may have arisen mainly due to the large eddies at the interface between the steam and water. The profiles appeared to be Gaussian in the region where the large eddies were observed, which were analogous to the observations in the earlier studies (Olsen & Dutton, 2003) with the inclusion of few maxima on both sides of the profiles, as seen in Figure 7.

It can be seen that with rising pressure, the PDF analysis reveal that the density of the instantaneous fluctuations has been raised in the core region all the way till the outer boundary of the core region not only in terms of the number of these fluctuations but also by the amplitudes of their fluctuations as well. The entrainment inhibited by the variation of the inlet pressure has been investigated using the measurements for the vortices following the equation,

$$\omega = \frac{\partial V_r}{\partial y} - \frac{\partial V_y}{\partial r} \qquad (1)$$

as well as in parallel measurements for the extent of the swirling strengths (Khan *et. al.*, 2020) for comparison. The contours of these vorticities again were estimated by the given equation and these values were normalized by the exit velocities before being plotted, as shown in Figure 8. These plots have been transformed into black and white contours with the help of

the contrast preserving decolorization (Zhao *et. al.*, 2018) and then the Matlab-based edge detection technique (Matlab, n.d.). The finally transformed contours are presented on a plot consisting of the vertical and the radial distances as shown in Figure 8. At lower pressure, the steam jet has shown a penetrating profile over a core region in the water in the vertically upward direction, whereas the jet profile diverges outward slightly when the jet raises further up into the water. This may probably be due to the

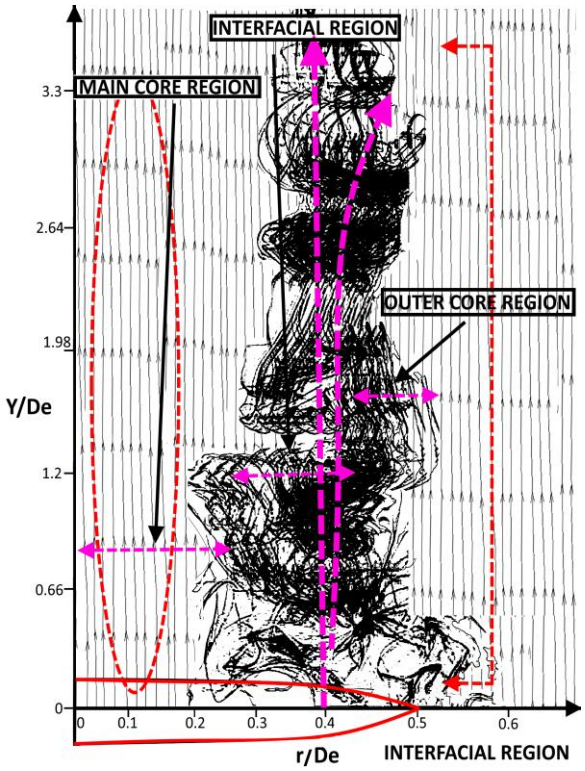

Fig. 8. Vorticity Profiles across the shear layer.

repetitive inception and collapse of the steam bubbles and subsequent filling of the voidages by the surrounding water, with its sudden expulsion towards the surroundings. The pressure recovery at the nozzle exit from lower pressure to the ambient due to the sudden expansion of steam jet may involve several factors and the physics of the phenomena is indeed complex to describe.

In the case of the lower inlet pressure, the vorticities were confined within a narrow strip of spatial width and they expanded vertically up in the water. At the lower pressure, the width of this strip was larger corresponding to the lower penetration length, whereas, in the case of the higher inlet pressure this strip expanded in the water, thus more radial penetration was observed, with lower vertical penetration for the supersonic steam jet at lower inlet pressure. In addition to it, the vertical structures possessed less density within the central core, with more density being concentrated within the outer region as highlighted by the division of the vorticities on both sides of the vertically segregating line in Figure 8. This finding supported earlier research in this regard in which the higher entrainment was attributed to the lower inlet pressure as well as Mach number at a fixed penetration distance, which was found by the planar velocity measurements in compressible mixing layers . The width of the spatial plane having vorticities contained within it may be attributed to the extent of entrainment, thus at a lower inlet pressure at a fixed penetration length, higher penetration would take place in the surrounding water.

4. Conclusion

An experimental study involving injection of the supersonic steam jet into the subcooled water was performed and the flow dynamics were carefully studied within the region close to the supersonic steam's exit from the nozzle. It was found that the radial spread of the steam's jet at the nozzle's exit was minor and the jet's velocity in the core region of the plume didn't change much till Y/De ~ 4.3. Whereas, the vertically upward of jet's exit velocity gradually decreased till Y/De ~ 8, however, the jet's normalized velocity achieved an optimized value between Y/De ~ 8 and Y/De ~ 9.8. Another interesting outcome was observed that with varying the pressure from 1.5 bars to 3.0 bars, the jet expanded radially in water at atmospheric pressure. Also, the asymmetric profile was observed right at the jet's exit and even the asymmetric profile also propagated further downstream of the nozzle exit. Also, the shear layer's width increased gradually, however, the shear thickness remained within 0.2 – 0.5 De over the 1.5 – 3.0 bars pressure. The normalized normal stresses, along with the normalized horizontal distances at lower pressure, were accrued in the region where the shear layer occurred, and propagated, and along the axial direction, both Reynolds shear and normal

stresses increased with higher amplitudes. PDF analysis showed that the velocity fluctuations across the shear layer were due to the large eddies across the steam-water interface and their profiles were found to be Gaussian. With increase in inlet pressure, the PDF analysis revealed the density of the velocity fluctuations were raised within the core region. Transformation of the vortical contours by the application of contrast preserving decolorization into black and white contours indicates that at lower pressure, the steam jet profile was penetrating over a core region in the water along vertically upward direction.

ACKNOWLEDGEMENTS

The authors are thankful to the Russian Government and Institute of Engineering and Technology, Department of Hydraulics and Hydraulic and Pneumatic Systems, South Ural State University, Lenin prospect 76, Chelyabinsk, 454080, Russian Federation for their support to this work through Act 211 Government of the Russian Federation, contract No. 02. A03.21.0011.

References

Afrasyab, K., Sanaullah, K., Takriff, M.S., Zen, H., Fong, L.S., **(2013).** Inclined Injection of Supersonic Steam into Subcooled Water: A CFD Analysis. Adv. Mater. Res. 845, 101–107. doi:10.4028/www.scientific.net/AMR.845.101

Ben-Yakar, A., Mungal, M.G., Hanson, R.K., (2006). Time evolution and mixing characteristics of hydrogen and ethylene transverse jets in supersonic crossflows. Phys. Fluids 18, 026101. doi:10.1063/1.2139684

Brown, G.L., Roshko, A., (1974). On density effects and large structure in turbulent mixing layers. J. Fluid Mech. 64, 775–816. doi:10.1017/S002211207400190X

Cattafesta, L., Alvi, F., Williams, D., Rowley, C., (2003). Review of Active Control of Flow-Induced Cavity Oscillations (Invited). American Institute of Aeronautics and Astronautics (AIAA). doi:10.2514/6.2003-3567

Chun, M.H., Kim, Y.S., Park, J.W., (1996). An investigation of direct condensation of steam jet in subcooled water. Int. Commun. Heat Mass Transf. 23, 947–958. doi:10.1016/0735-1933(96)00077-2

Davidenko, D., Gökalp, I., Dufour, E., Magre, P., (2003). Numerical simulation of hydrogen supersonic combustion and validation of computational approach, in: 12th AIAA International Space Planes and Hypersonic Systems and Technologies. doi:10.2514/6.2003-7033

Furudate, M., Lee, B.J., Jeung, I.S., (2005). Computation of HyShot scramjet flows in the T4 experiments, in: A Collection of Technical Papers - 13th AIAA/CIRA International Space Planes and Hypersonic Systems and Technologies Conference. pp. 1419–1428. doi:10.2514/6.2005-3353

Gardner, A.D., Hannemann, K., Paull, A., Steelant, J., (2005). Ground testing of the HyShot supersonic combustion flight experiment in HEG, in: Shock Waves. Springer Berlin Heidelberg, pp. 329–334. doi:10.1007/978-3-540-27009-6_47

Gruber, M.R., Nejadt, A.S., Chen, T.H., Dutton, J.C., (1995). Mixing and penetration studies of sonic jets in a mach 2 freestream. J. Propuls. Power 11, 315–323. doi:10.2514/3.51427

Kaufman, L.G., (1967). Hypersonic flows past transverse jets. J. Spacecr. Rockets 4, 1230–1235. doi:10.2514/3.29057

Khan, A., (2014). CFD Based Hydrodynamic Parametric Study of Inclined Injected Supersonic Steam into Subcooled Water. doi:10.3850/978-981-09-4587-9_P03

Khan, A., Sanaullah, K., Haq, N.U., (2013). Development of a Sensor to Detect Condensation of Super-Sonic Steam. Adv. Mater. Res. 650, 482–487. doi:10.4028/www.scientific.net/AMR.650.482

Khan, A., Sanaullah, K., Sobri Takriff, M.,

Hussain, A., Shah, A., Rafiq Chughtai, I., (2016). Void fraction of supersonic steam jet in subcooled water. Flow Meas. Instrum. 47, 35–44.doi:10.1016/J.FLOWMEASINST.2015.12.002

Khan, A., Takriff, M.S., Rosli, M.I., Othman, N.T.A., Sanaullah, K., Rigit, A.R.H., Shah, A., Ullah, A., Mushtaq, M.U., (2019). Turbulence dissipation & its induced entrainment in subsonic swirling steam injected in cocurrent flowing water. Int. J. Heat Mass Transf.145,118716.doi:10.1016/J.IJHEATMASSTRANSFER.2019.118716

Khan, A., Takriff, M.S., Sanaullah, K., Zwawi, M., Algarni, M., Felemban, B.F., Bahadar, A., Shah, A., Rigit, A.R.H., (2020). Periodic compression and cavitation induced shear between steam-water two-phase flows for bio-materials degradation. Int. J. Environ. Sci. Technol. 17, 1591–1626. doi:10.1007/s13762-019-02601-2

Ko, H., Yoon, W.S., (2002). Performance analysis of secondary gas injection into a conical rocket nozzle. J. Propuls. Power 18, 585–591. doi:10.2514/2.5972

Larson, W.J., Henry, G.N., Humble, R.W., (1995). Space propulsion analysis and design. McGraw-Hill.

Martinez Schramm, J., Karl, S., Hannemann, K., Steelant, J., (2008). Ground testing of the HyShot II scramjet configuration in HEG, in: 15th AIAA International Space Planes and Hypersonic Systems and Technologies Conference. doi:10.2514/6.2008-2547

Matlab, n.d. Find edges in intensity image - MATLAB edge [WWW Document]. URL https://www.mathworks.com/help/images/ref/edge.html.

Mi, J., Kalt, P., Nathan, G.J., Wong, C.Y., (2007). PIV measurements of a turbulent jet issuing from round sharp-edged plate. Exp. Fluids 42, 625–637. doi:10.1007/s00348-007-0271-9

Olsen, M.G., Dutton, J.C., (2003). Planar velocity measurements in a weakly compressible mixing layer. J. Fluid Mech. 486, 51–77. doi:10.1017/S0022112003004403

Papamoschou, D., Roshko, A., (1988). The compressible turbulent shear layer: An experimental study. J. Fluid Mech. 197, 453–477. doi:10.1017/S0022112088003325

Rowley, C.W., Williams, D.R., (2006). DYNAMICS AND CONTROL OF HIGH-REYNOLDS-NUMBER FLOW OVER OPEN CAVITIES. Annu. Rev. Fluid Mech. 38, 251–276. doi:10.1146/annurev.fluid.38.050304.092057

Sarno, R.L., Franke, M.E., (1994). Suppression of flow-induced pressure oscillations in cavities. J. Aircr. 31, 90–96. doi:10.2514/3.46459

Solovitz, S.A., Mastin, L.G., Saffaraval, F., (2011). Experimental study of near-field entrainment of moderately overpressured jets. J. Fluids Eng. Trans. ASME 133. doi:10.1115/1.4004083

Song, Chul-Hwa; Cho, Seok; Kim, Hwan-Yeol; Bae, Yoon-Young; Chung, M.-K., (2007). THERMAL-HYDRAULIC TESTS AND ANALYSES FOR THE APR1400'S DEVELOPMENT AND LICENSING. Nucl. Eng. Technol. 39. doi:10.5516/NET.2007.39.4.299

Song, Chul-Hwa; Cho, Seok; Kim, Hwan-Yeol; Bae, Yoon-Young; Chung,. (2000). Characterization of direct contact condensation of steam jets discharging into a subcooled water (Conference) | ETDEWEB [WWW Document]. URLhttps://www.osti.gov/etdeweb/biblio/20071733.

Turner, J.S., (1986). Turbulent entrainment: The development of the entrainment assumption, and its application to geophysical flows. J. Fluid Mech. 173, 431–471. doi:10.1017/S0022112086001222

Ukeiley, L.S., Ponton, M.K., Seiner, J.M., Jansen, B., (2004). Suppression of pressure loads in cavity flows. AIAA J. 42, 70–79. doi:10.2514/1.9032

Urban, W.D., Mungal, M.G., (1997). Planar velocity measurements in compressible mixing layers, in: 35th Aerospace Sciences Meeting and Exhibit. American Institute of Aeronautics and Astronautics Inc, AIAA. doi:10.2514/6.1997-757

US7842264B2 – (2008) Process and apparatus for carbon capture and elimination of multi-pollutants in flue gas from hydrocarbon fuel sources and recovery of multiple by-products - Google Patents [WWW Document], n.d. URL https://patents.google.com/patent/US7842264B2/en.

Vakili, A.D., Gauthier, C., (1994). Control of cavity flow by upstream mass-injection. J. Aircr. 31, 169–174. doi:10.2514/3.46470

Vanierschot, M., Persoons, T., Van den Bulck, E., (2009). A new method for annular jet control based on cross-flow injection. Phys. Fluids 21, 025103. doi:10.1063/1.3037343

Weimer, J.C., Faeth, G.M., Olson, D.R., (1973). Penetration of vapor jets submerged in subcooled liquids. AIChE J. 19, 552–558. doi:10.1002/aic.690190321

Wu, X.Z., Yan, J.J., Pan, D.D., Liu, G.Y., Li, W.J., (2009). Condensation regime diagram for supersonic/sonic steam jet in subcooled water. Nucl. Eng. Des. 239, 3142–3150. doi:10.1016/j.nucengdes.2009.08.010

Wu, X.Z., Yan, J.J., Shao, S.F., Cao, Y., Liu, J.P., (2007). Experimental study on the condensation of supersonic steam jet submerged in quiescent subcooled water: Steam plume shape and heat transfer. Int. J. Multiph. Flow 33, 12961307.doi:10.1016/j.ijmultiphaseflow.2007.06.004

Zakkay, V., Calarese, W., Sakell, L., (1971). An experimental investigation of the interaction between a transverse sonic jet and a hypersonic stream. AIAA J. 9, 674–682. doi:10.2514/3.6247

Zhao, H., Zhang, H., Jin, X., (2018). Efficient image decolorization with a multimodal contrast-preserving measure. Comput. Graph. 70, 251–260. doi:10.1016/j.cag.2017.07.009

Zukoski, E.E., Spaid, F.W., (1964). Secondary injection of gases into a supersonic flow. AIAA J. 2, 1689–1696. doi:10.2514/3.2653

Submitted: 22/07/2020

Revised: 19/10/2020

Accepted: 26/10/2020

DOI: 10.48129/kjs.v48i4.10214